

Supporting Information

Gandhi et al. 10.1073/pnas.0806159105

SI Methods

Hebbian Model of Delayed Inhibitory Plasticity. The model describes the normalized responses of two cells, one excitatory, F_e , and one inhibitory, F_i , as the linear sum of their inputs:

$$F_e(t) = W_{de}(t)E_d(t) + W_{oe}(t)E_o(t) - W_{ie}F_i(t)$$

$$F_i(t) = W_{di}(t)E_d(t) + W_{oi}(t)E_o(t) + W_{ei}F_i(t),$$

where E_d represents inputs activated by the deprived eye, E_o represents inputs activated by the open eye, and the matrix W contains the weights of the connections shown in Fig. 4A. To describe the learning rule for each connection following monocular deprivation, we used a Hebbian covariance rule (1):

$$\frac{dW_{de}(t)}{dt} = K_{de} \langle E_d(t), (F_e(t) - F_e) \rangle$$

1. Dayan P, Abbott LF (2001) *Theoretical Neuroscience* (MIT Press, Cambridge, MA), 1st Ed.

$$\frac{dW_{di}(t)}{dt} = K_{di} \langle E_d(t), (F_i(t) - F_i) \rangle,$$

where F represents the averaged ongoing activity for the neuron before deprivation, and K sets the connection-specific learning rate. The remaining connection weights were held fixed:

$$\frac{dW_{ei}(t)}{dt} = \frac{dW_{ie}(t)}{dt} = \frac{dW_{oi}(t)}{dt} = \frac{dW_{oe}(t)}{dt} = 0.$$

The weights of the nondeprived connections (W_{oi} and W_{oe}) were fixed because our experimental results indicate that nondeprived eye responses in both populations do not change substantially during the initial phase of plasticity. The weights of the local connections (W_{ie} and W_{ei}) were held fixed to examine the dependence of inhibitory and excitatory cell plasticity on the strength of these connections.

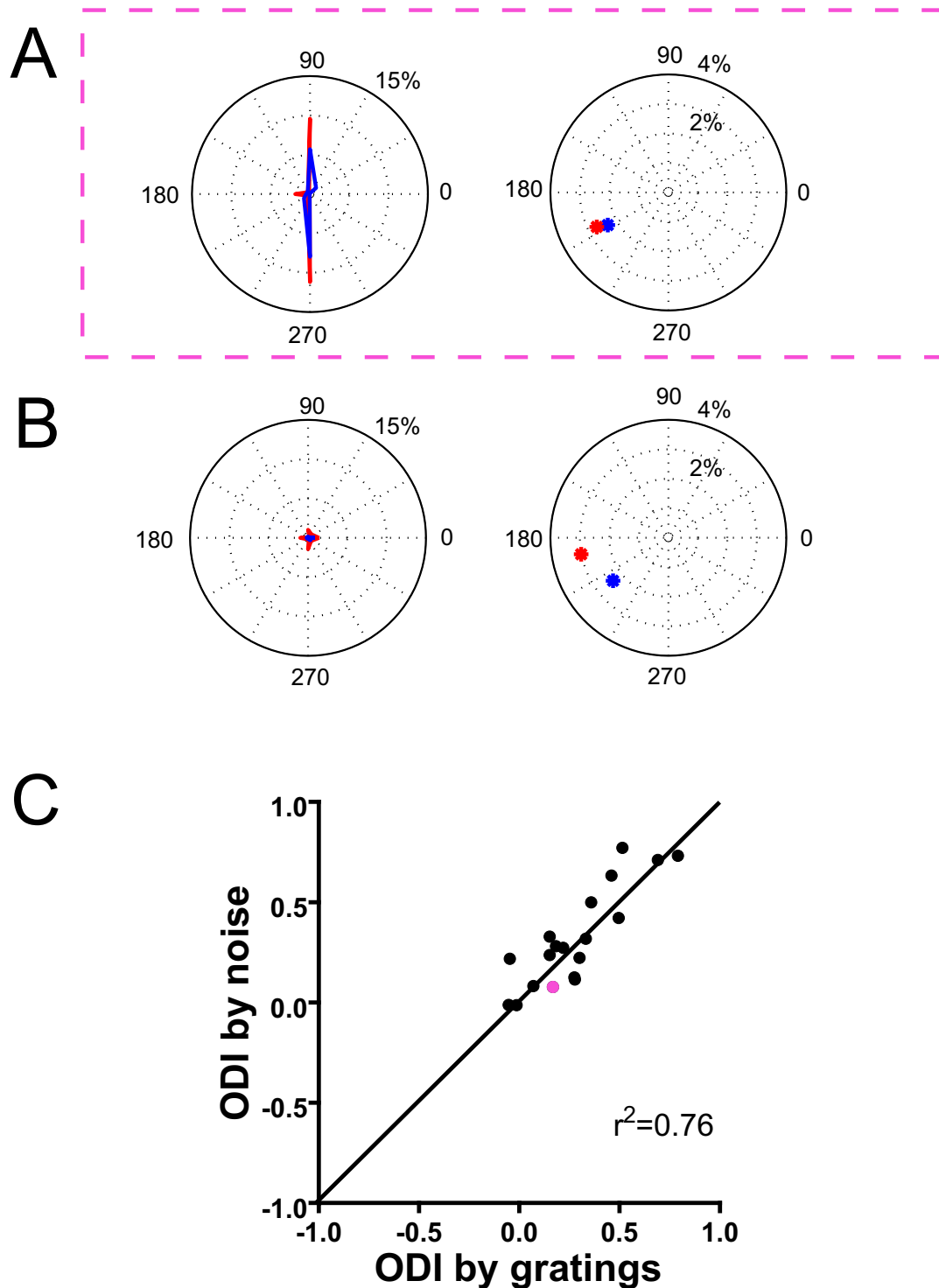


Fig. S1. Ocular dominance determined by noise stimulation matches that determined by using conventional, drifting grating stimuli. (*A Left*) Example orientation selective response of a neuron from the binocular zone of mouse primary visual cortex, plotting average response ($\Delta F/F$) to 10 presentations of a sinusoidal drifting grating stimulus (4 Hz; 0.05 cycles per degree) presented at 8 orientations (0–315°). Red shows average response to contralateral-eye stimulation, and blue shows ipsilateral-eye response. (*A Right*) For the same cell in *Left*, magnitude and phase of response evoked by the contrast modulated stochastic noise stimulus presented to the contralateral (red) and ipsilateral (blue) eye. The ODI values obtained by using these two techniques are similar (see magenta in *C*). (*B*) Example of neuron that responds poorly when grating stimuli are presented to each eye (10 of 28 cells) but responds well to stochastic noise stimulus. (*C*) For cells that responded well to the grating stimuli (18 of 28), the ODI obtained by the noise stimulus was similar ($r^2 = 0.76$).

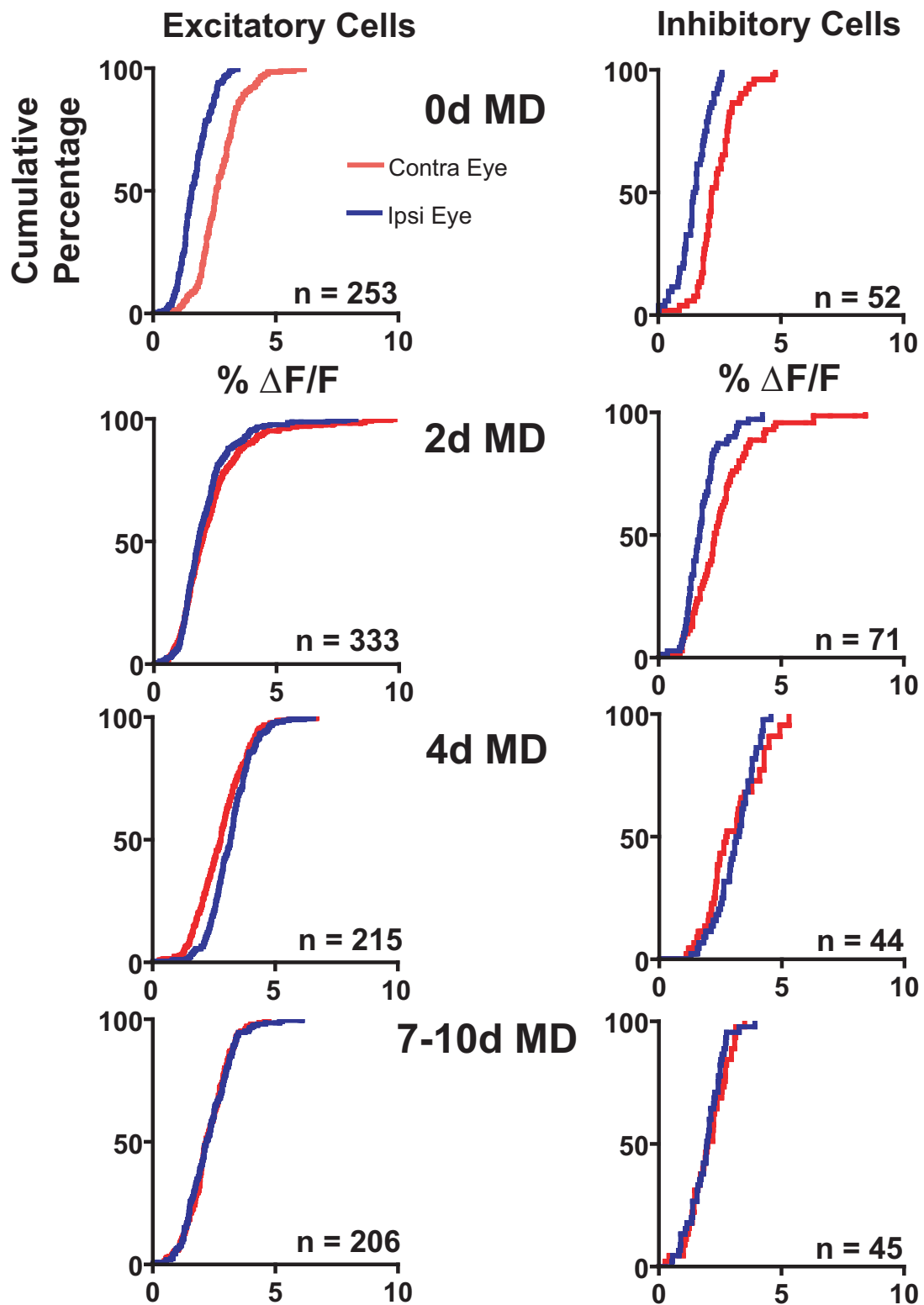
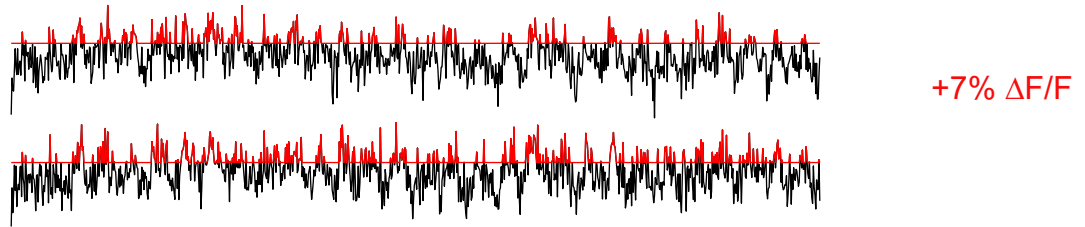


Fig. S2. Cumulative plots of contralateral and ipsilateral eye responses from excitatory and inhibitory cells across all groups.

A



B

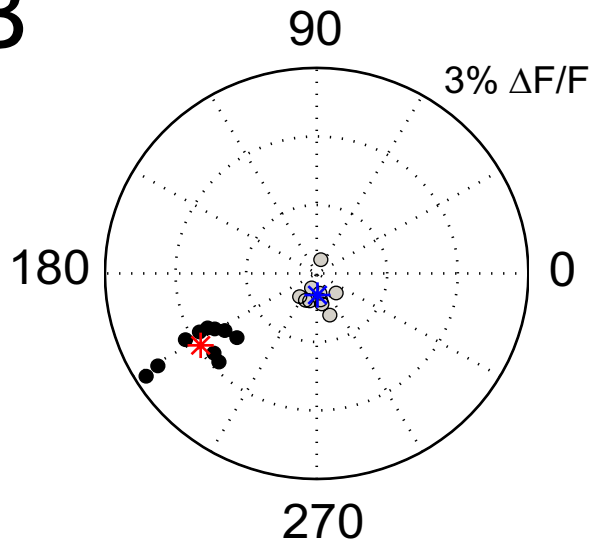
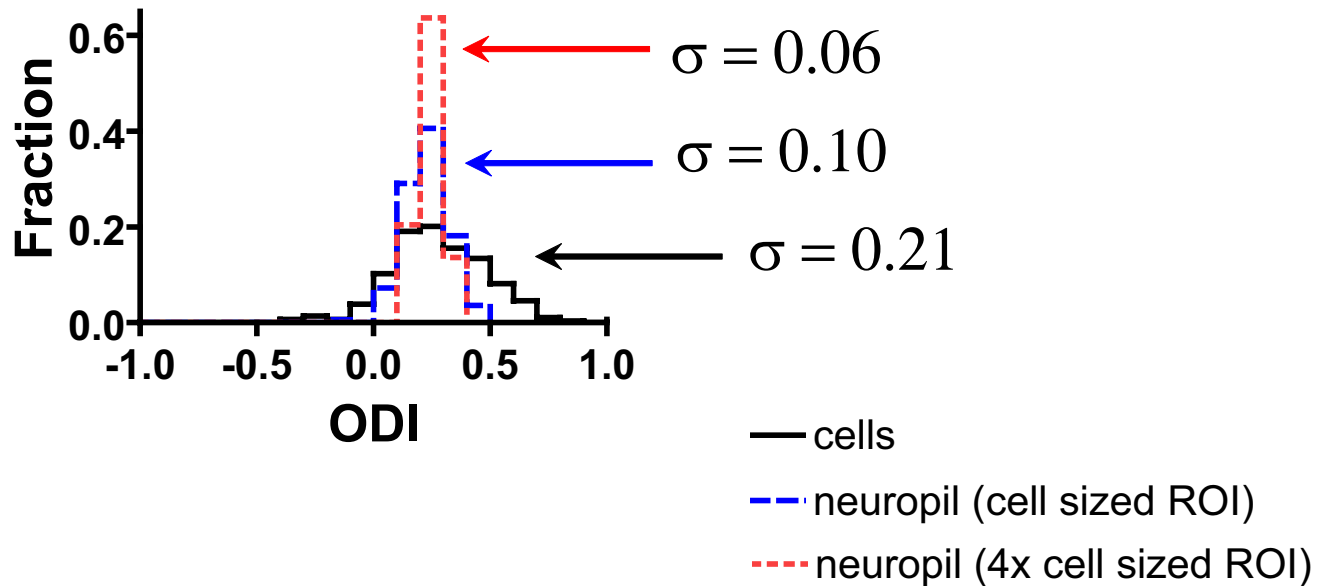


Fig. S3. Responses to contrast noise stimuli are generated by suprathreshold calcium transients and not subthreshold variation. Calcium signals recorded in neuronal cell bodies predominantly reflect spiking activity (1–3) with calcium indicator transients observed as high as 15% per spike. To determine whether the modest (1–5%; see Fig. S2) signal modulations that are the result of our Fourier analysis of the noise responses are generated by large calcium transients and are not the result of hitherto undetected, small subthreshold calcium signals, we clipped the responses shown in Fig. 2 with a 7% threshold, which should include only suprathreshold signals, and then performed our analysis again. (A) Red shows the results of clipping sample traces at a 7% $\Delta F/F$ threshold (peak-to-trough). Considerable periodic modulation above the threshold is apparent. (B) Responses of all 10 cells (shown in B) computed from clipped traces remain well separable from the no-stimulation condition.

1. Ohki K, et al. (2005) Functional imaging with cellular resolution reveals precise micro-architecture in visual cortex. *Nature* 433:597–603.
2. Mrsic-Flogel TD, et al. (2007) Homeostatic regulation of eye-specific responses in visual cortex during ocular dominance plasticity. *Neuron* 54:961–972.
3. Sohya K, et al. (2007) GABAergic neurons are less selective to stimulus orientation than excitatory neurons in layer II/III of visual cortex, as revealed by in vivo functional Ca^{2+} imaging in transgenic mice. *J Neurosci* 27:2145–2149.

A 0 days monocular deprivation



B 7 days monocular deprivation

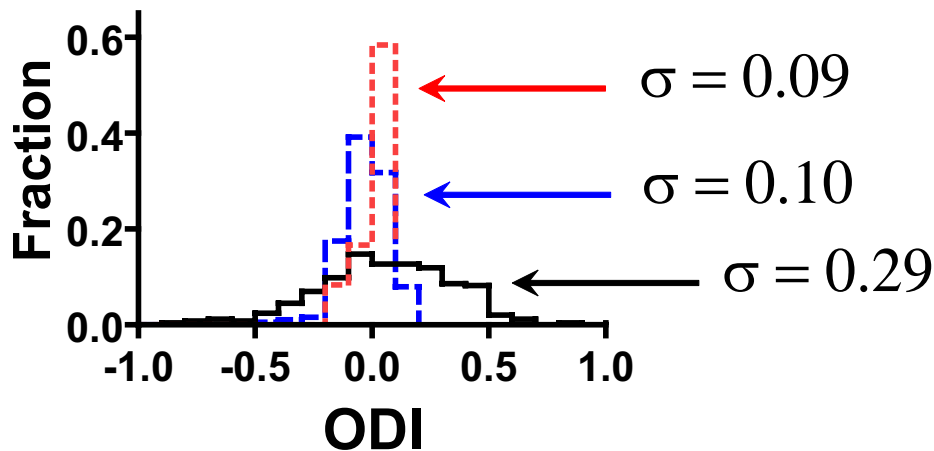


Fig. S4. Signals from the neuropil are homogeneous and reflect average cell activity, highlighting the importance of excluding neuropil from cellular recordings. (A) ODI distributions of responses from cell bodies (black), and from small (blue) and large (red) regions of neuropil surrounding the recorded cells. Signals pooled over cell-sized regions of neuropil are considerably more homogeneous than the cell responses themselves in control animals. Increasing the size of the neuropil regions further narrowed the response distribution. (B) A similar pattern was found in recordings from the 7- 10-day MD group.

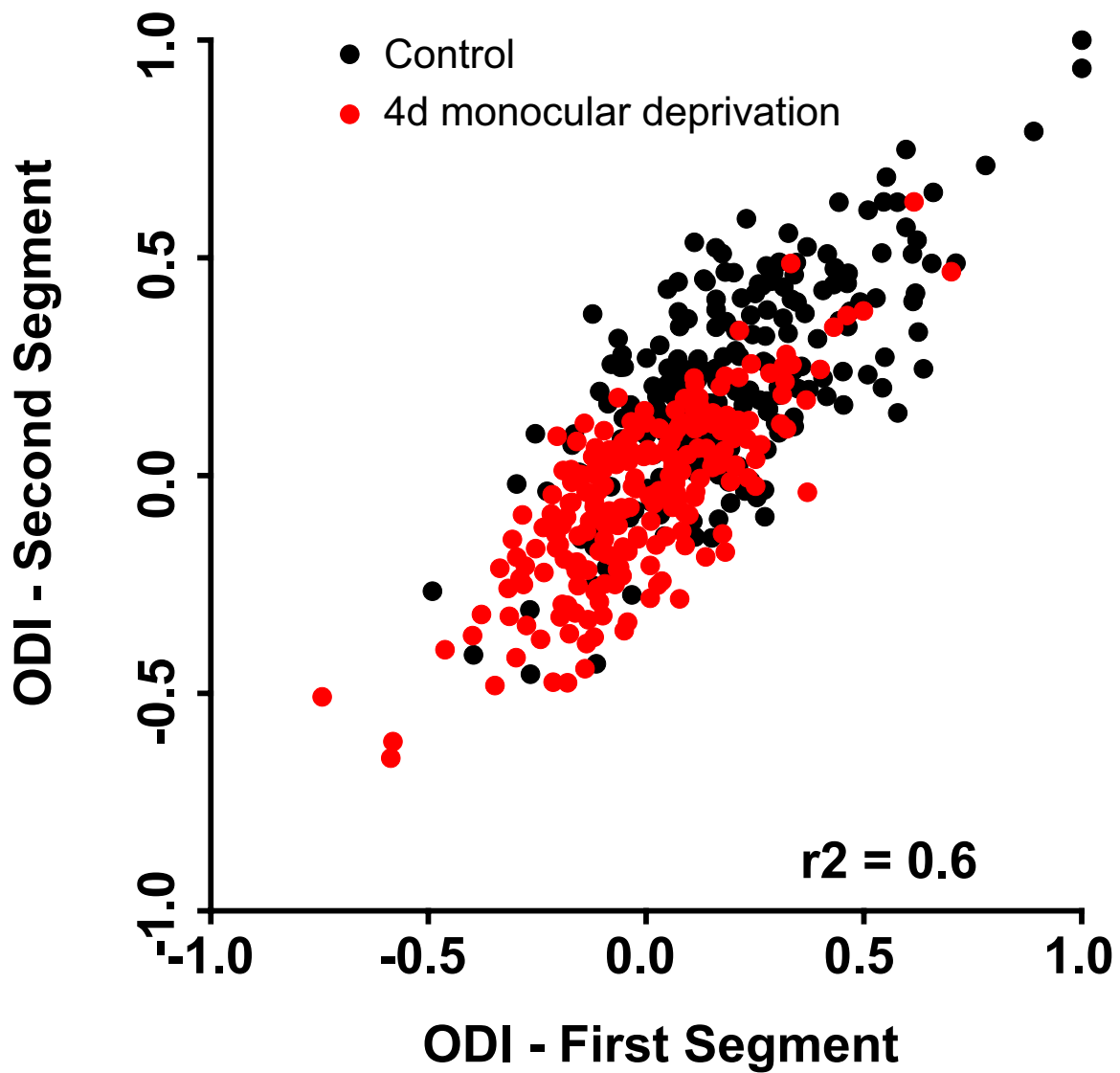


Fig. S5. Broad distribution of ODI reflects cell-by-cell response specificity rather than measurement error. Calcium indicator response traces from nondeprived (black) and 4-day MD (red) groups were divided into two segments and ODIs for each cell were computed separately for each segment. The two determinations of ocular dominance for each cell were well correlated ($r^2 = 0.6$). This correlation indicates that despite the increased measurement noise resulting from halving the response data, most of the variance in the distribution of measured ocular dominance is because of real differences among cells and not because of measurement error.

